ELSEVIER

Materials Science and Engineering B 130 (2006) 269–272

MATERIALS SCIENCE & ENGINEERING B

www.elsevier.com/locate/mseb

Study on the Raman scattering measurements of Mn ion implanted GaN

Y.H. Zhang *, L.L. Guo, W.Z. Shen

Laboratory of Condensed Matter Spectroscopy and Opto-Electronic Physics, Department of Physics, Shanghai Jiao Tong University, 1954 Hua Shan Road, Shanghai 200030, PR China

Received 9 October 2005; accepted 19 March 2006

Abstract

We investigate the temperature dependent Raman spectra of Mn implanted (Ga,Mn)N samples with five Mn implantation doses. A small shoulder at 572.4 cm^{-1} on the high energy side of the main Raman peak E_2^H has been attributed to the Mn-related local vibrational mode (LVM). It is found that with the increase of Mn implantation dose the intensity ratio of LVM to that of the E_2^H ($I_{LVM}/I_{E_2^H}$) increases at first and tends to saturate at high implantation dose. In addition, at high temperature or after rapid thermal anneal treatment, the value of $I_{LVM}/I_{E_2^H}$ decreases significantly, explaining the reason why it is difficult to observe Mn-related LVM reported in the literature.

Keywords: Diluted magnetic semiconductors; Raman spectra; Local vibrational mode

After the realization of (In,Mn)As and (Ga,Mn)As [1,2], more and more efforts have been devoted to (Ga,Mn)N diluted magnetic semiconductors (DMS) that exploit the charge and the spin of electrons [3] because of the following two important reasons. Firstly, GaN-based III–V semiconductors have potential applications in electronic and optoelectronic device, such as blue-ultraviolet light-emitting diodes, and laser diodes [4–6]. Secondly, from the viewpoint of applications of DMS, it is desirable to find materials with Curie temperature as high as possible and one of the recent theoretical works [7] has shown that wide band gap semiconductors, GaN and ZnO, may be possible to realize ferromagnetism at room temperature or higher. Although some experimental studies on the magnetic characteristics of GaN-based DMS have been reported [8–12], there are many fundamental properties, especially the magnetic ion related properties, about (Ga,Mn)N still not clear and need to be investigated deliberately.

Raman scattering is a standard optical characterization technique for studying various fundamental aspects of solids such as lattice and electronic properties. First Raman scattering study of (Ga,Mn)N alloy with Mn concentration lower than 2% was performed by Gebicki et al. [13]. A very weak Raman band on the high energy side of E_2^H was observed, which they considered to be the Mn-related local vibrational mode (LVM), however, the detailed behavior of LVM has not been demonstrated yet. Other investigations about the Raman spectra of ion implanted (Ga,Mn)N system only presented some conventional bands, which could also be observed in GaN-based semiconductor doped with non-magnetic ion species and was certainly independent of the specific Mn ion [9]. In fact, study on the (Ga,Mn)N system with high Mn concentration is more interesting and preferred, because the high magnetic ion concentration is desired in DMS material. Nevertheless, detailed Raman scattering studies on the (Ga,Mn)N system with high Mn concentration are seldom available in the literature up to now, especially the magnetic Mn ion related Raman behavior has not been studied in detail yet. In this paper, the temperature dependent micro-Raman spectra of Mn implanted (Ga,Mn)N samples with both low and high Mn concentrations were investigated. The Mn-related LVM was observed and investigated in detail.

The Si-doped GaN film was grown on (0 0 0 1) sapphire substrates by hydride vapor phase epitaxy (HVPE). The GaN epilayer shows *n*-type conductivity and the thickness is 3.8 μm. The as-grown sample was then cut into 10 equivalent pieces. Every two pieces were uniformly implanted with same Mn dose at a constant energy of 190 keV. Totally, we get 10 pieces of (Ga,Mn)N samples with five Mn implantation doses of 1, 3, 5, 7, and 9×10^{16} cm^{-2}, respectively, corresponding to approximately 1, 3, 5, 7, and 9% Mn concentration at the peak of the implant profile. To avoid amorphization during the implantation step, the samples were held at a temperature of 350 °C. After implantation, one piece of each implantation dose was selected

* Corresponding author. Tel.: +86 21 54743242; fax: +86 21 54741040.
E-mail address: yuehzhang@sjtu.edu.cn (Y.H. Zhang).

0921-5107/$ – see front matter © 2006 Elsevier B.V. All rights reserved.
doi:10.1016/j.mseb.2006.03.014

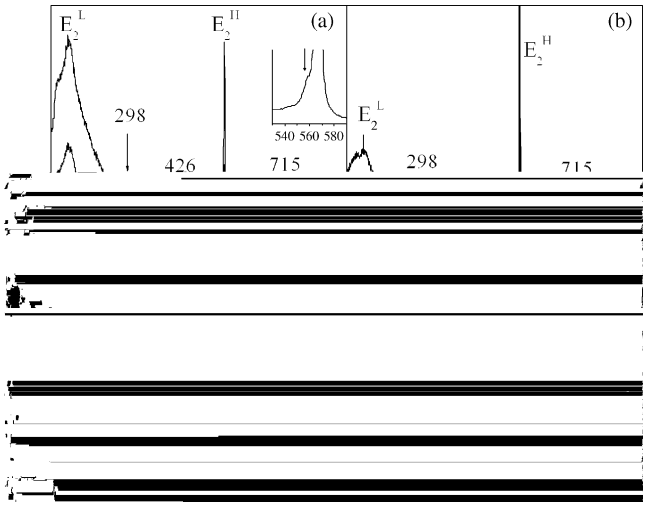

Fig. 1. The first-order Raman spectra of (a) as-implanted and (b) RTA samples with five different implantation doses at room temperature. The ion implantation dose from top to the bottom is 1, 3, 5, 7, and $9 \times 10^{16}\,cm^{-2}$, respectively. The Raman spectra of the GaN epilayer and the sapphire substrate are also displayed. The spectra have been shifted for clarity.

to deal with rapid thermal anneal (RTA) at 900 °C for 1 min, under flowing N_2 gas with implanted area face down. The quality of samples was studied by means of X-ray diffraction measurements. Only the peaks corresponding to GaN and sapphire were observed and no second phases of Ga_xMn_y were detected. The temperature dependent Raman measurements were carried out from 83 to 293 K using the 514.5 nm line of an Ar^+ laser as an excitation source. The laser beam was focused yielding a spot size of 1 μm. The scattered light was recorded in backscattering geometry using a Jobin Yvon LabRaman HR 800 UV micro-Raman spectrometer.

Fig. 1 shows the first-order Raman spectra of (a) as-implanted and (b) RTA (Ga,Mn)N samples with five different Mn implantation doses at room temperature. For comparison the Raman spectra of the as-grown GaN eplilayer and the sapphire substrate are also displayed. For the as-grown GaN eplilayer, the characteristic features of E_2^L, E_2^H and A_1(LO) peaks were clearly observed. In comparison with the spectrum of the sapphire substrate, we can distinguish the Raman signals from the sapphire substrate in the Raman spectrum of the as-grown GaN eplilayer [marked by asterisks at 379, 418, 431, 449, 577, and 750 cm^{-1} in Fig. 1(b)] due to the large penetrating depth of the 514.5 nm excitation laser. A small shoulder at 560 cm^{-1} on the low energy side of E_2^H is the E_1(TO) phonon, which is enlarged in the insert of Fig. 1(a). It is known that the E_1(TO) should be forbidden for a backscattering geometry. Its appearance stems from the small deviation from the backscattering configuration in the micro-Raman system.

After implantation, the Raman spectra differ considerably from the original as-grown GaN material. In addition to a strong amorphous background, some new bands centered around 298, 366, 426, 669, and 715 cm^{-1} occurred. According to the previous investigations about the GaN material implanted with other ion species [14–16], the band at 298 cm^{-1} is assigned to the highest acoustic phonon branch at zone boundary, 366 cm^{-1} is supposed to be vacancy complexes or dislocations, whereas the structure at 426 cm^{-1} results from two phonons difference mode and the band at 669 cm^{-1} is due to less complex defect. Though not reported in the literature, the band at 715 cm^{-1} agrees well with the phonon density of state of (Ga,Mn)N calculated with a rigid ion model by Gebicki et al. [17]. The corresponding Raman spectra after RTA process show that the intensity of these bands and the amorphous background decrease greatly in contrast to the increase of E_2^H, whereas the signals related with host GaN lattice increase obviously, indicating that RTA process recovers the crystalline structure significantly.

So far, only signals related to the host lattice have been described. In fact, we could also observe foreign signals induced by impurities. If impurity atom replaces host lattice atoms heavier than the impurities, atomic oscillation may be induced in a limited range around the impurities, which is so-called LVM. Its frequency appears in the energy gap between the acoustic and optical branches of phonon, or above the optical branch. Though it is recognized that in ion implantation system the implanted ion mainly occupy interstitial site at first, however, due to the fact that the samples were held at a temperature of 350 °C during fabrication and the implantation dose is high, it is possible that a certain amount of Mn ion occupy the Ga sites even before the RTA process. Therefore, Mn-related LVM should be considered. Assuming that Mn occupied a gallium site, the frequency of Mn in GaN matrix can be estimated with the simple mass defect approximation [18]:

$$\omega = \omega_{GaN}^{TO}\sqrt{\frac{\mu_{GaN}}{\mu_{MnN}}}$$

A LVM at 572.5 cm^{-1} is expected using $\omega = \omega[E_1(TO)] = 560\,cm^{-1}$. We note that the LVM is very close to the E_2^H, and it is difficult for us to observe such a LVM mode. Therefore, the Mn-related LVM was seldom studied in detail up to now. To investigate the behavior of Mn-related LVM more clearly, we will concentrate on the spectra range 550–590 cm^{-1} in the following.

In Fig. 2(a), the experimental Raman spectra of as-implanted (Ga,Mn)N with different Mn implantation doses at 83 K are displayed as solid circles. The small shift of E_2^H with implantation dose may result from strain. It is known that lattice structure may be distorted in the neighborhood of native defects or by incorporated impurities. These point defects will induce a three-dimension strain such as hydrostatic stress if the defects are uniformly distributed. A small shoulder at ~572.4 cm^{-1} on the high energy side of E_2^H can be clearly observed at each kind of implantation dose, which coincides exactly with the frequency of the calculated Mn LVM. Because this shoulder cannot be found in the Raman spectrum of the as-grown GaN epilayer at any temperature, it results from Mn implantation. Furthermore, the relative ratio of the intensity of this structure to that of the E_2^H changes with the Mn implantation dose. Therefore, we assign this structure to the Mn-related LVM. To investigate the behavior of the LVM quantitatively, we fitted the Raman spectra with Lorentz model. As stated above, E_1(TO) phonon occurs close to the low energy side of E_2^H.So three Raman peaks should be

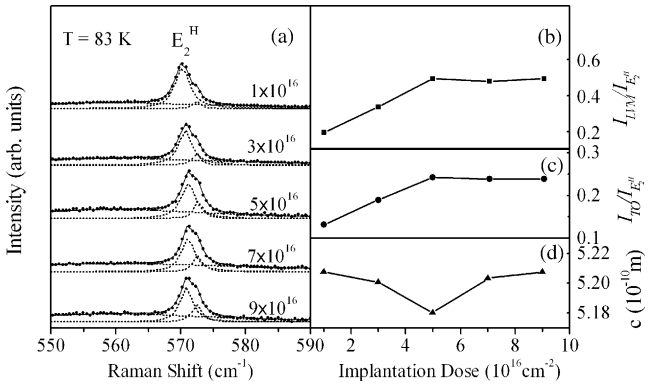

Fig. 2. (a) Experimental (solid circles) Raman spectra of as-implanted (Ga,Mn)N for different Mn implantation doses at 83 K. The solid curves are Raman spectra fitted with Lorentz model with the dotted curves for E_1(TO), E_2^H and the LVM mode. Dependence of the relative intensity ratio of the LVM (b) and E_1(TO) (c) to that of the E_2^H on the Mn implantation dose. (d) Dependence of the c-plane lattice constant derived by XRD measurement on the Mn implantation dose.

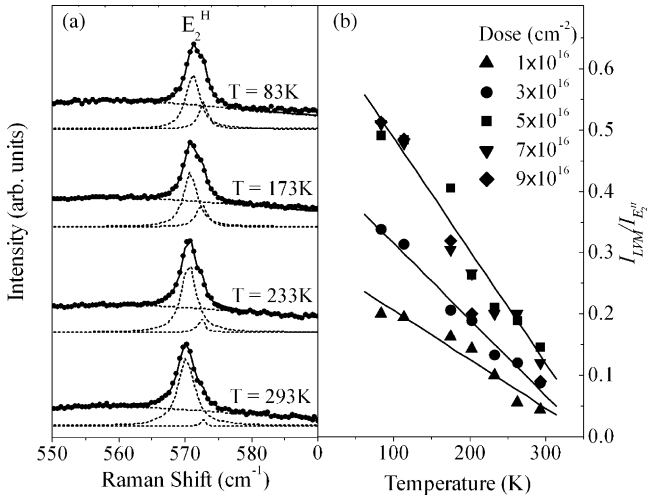

Fig. 3. (a) Experimental (solid circles) Raman spectra of as-implanted (Ga,Mn)N with Mn implantation dose of 5×10^{16} cm^{-2} at different temperatures. The solid curves are Raman spectra fitted with Lorentz model with the dotted curves for E_1(TO), E_2^H and the LVM mode. (b) Dependence of the relative intensity ratio $I_{LVM}/I_{E_2^H}$ on temperature in all the as-implanted samples. The solid curves are guide for eyes.

considered simultaneously, i.e. E_1(TO), E_2^H and the LVM mode, in this spectra range. Through fitting, we can obtain the Raman shift, the intensity and width of the three peaks. It is clear that the fitted results (solid curves) agree well with the experimental data.

The relative intensity ratios of the LVM and E_1(TO) to that of the E_2^H($I_{LVM}/I_{E_2^H}$ and $I_{TO}/I_{E_2^H}$) have been shown in Fig. 2(b) and (c). We observe that both $I_{LVM}/I_{E_2^H}$ and $I_{TO}/I_{E_2^H}$ have similar behavior with the Mn implantation dose. The ratios increase monotonically with Mn implantation dose at first and gradually saturate at high dose (5×10^{16} cm^{-2}). The dependence of $I_{LVM}/I_{E_2^H}$ on Mn implantation dose is easy to be understood. With the increase of Mn dose, more and more Mn replaces the gallium site, resulting in the enhancement of Mn-related LVM Raman signal. Further increase of the dose, however, Mn may incorporate as interstitially, leading to the saturation of $I_{LVM}/I_{E_2^H}$. This result suggests that the maximum solubility for substitution Mn in (Ga,Mn)N is about 5%, which agrees well with result of the c-plane lattice constants determined from XRD measurement, as shown in Fig. 2(d). The lattice constant decreases with the increase of Mn implantation dose and reaches the smallest at Mn implantation dose of 5×10^{16} cm^{-2}, corresponding to 5% Mn concentration. Similar results were also reported by Thaler et al. [19], Dhar et al. [20] and Chang et al. [21]. They considered that the decrease of the lattice constants is due to incorporation of Mn substitutionally on the Ga sites. Therefore, Fig. 2(d) also suggests the maximum for complete Mn substitutionality is 5%. As for the dependence of Mn implantation dose on $I_{TO}/I_{E_2^H}$, it is expected that more residual damage exists in the implanted material with increasing implantation dose. This phenomenon has also been reported by many authors in investigating Mn implanted GaAs [22], where the intensity ratio of I_{TO}/I_{LO} was used as a measure of the damage degree.

Fig. 3(a) displays experimental Raman spectra (solid circles) of the as-implanted sample with Mn implantation dose of 5×10^{16} cm^{-2} under different temperatures. All the spectra are again fitted with Lorentz model as solid curves. It is found that $I_{LVM}/I_{E_2^H}$ decreases with increasing temperature. We have shown in Fig. 3(b) the results of $I_{LVM}/I_{E_2^H}$ as a function of temperature in all the as-implanted samples. The data of $I_{LVM}/I_{E_2^H}$ at different implantation doses follow the similar linear dependence on temperature. When the implantation dose is larger than 5×10^{16} cm^{-2}, the values of $I_{LVM}/I_{E_2^H}$ at a fixed temperature almost merge together, which is consistent with the results of Fig. 2(b). It is known that Mn only partially replaces the gallium site. With temperature increasing, the intensity of the Mn-related LVM mode is enhanced not as obviously as that of E_2^H, which is closely related to the total host lattice. We therefore expect a decrease in $I_{LVM}/I_{E_2^H}$. It may be the similar reason that $I_{LVM}/I_{E_2^H}$ of the RTA samples is smaller than that of the as-implanted samples. Take the sample with Mn implantation dose of 5×10^{16} cm^{-2} as an example, the $I_{LVM}/I_{E_2^H}$ value of RTA sample at 83 K is only 0.07, which is much smaller than that of the corresponding as-implanted sample (0.49). After RTA treatment, the crystalline structure is recovered significantly, resulting in the enhancement of E_2^H and LVM. However, due to the fact that Mn only partially substitutes the gallium site, the enhancement of the Mn-related LVM mode resulted from the structure recovery is less significant compared with E_2^H, leading to the smaller $I_{LVM}/I_{E_2^H}$. These results explain why it is difficult to observe the Mn-related LVM for the RTA samples or in the case of high temperature in the literature.

In summary, the temperature dependent micro-Raman spectra were performed on Mn implanted (Ga,Mn)N samples with five different implantation doses. In addition to some conventional bands that were also observed in GaN-based semiconductor doped with other non-magnetic ion species, a small shoulder at 572.4 cm^{-1} was observed which we assign to LVM of Mn. The

intensity ratio $I_{\mathrm{LVM}}/I_{E_2^{\mathrm{H}}}$ increases monotonically with increasing Mn implantation dose at first and then tends to saturate at high dose ($>5 \times 10^{16}\,\mathrm{cm}^{-2}$), suggesting the 5% maximum solubility for substitution Mn in (Ga,Mn)N. With temperature increasing or after RTA process, the value of $I_{\mathrm{LVM}}/I_{E_2^{\mathrm{H}}}$ decreases, explaining the difficulty in observing the Mn-related LVM in the literature.

Acknowledgement

This work is supported in part by the Natural Science Foundation of China under Contracts no. 10304010 and 10125416.

References

[1] H. Munekata, H. Ohno, S. von Molnar, A. Segmuller, L.L. Chang, L. Esaki, Phys. Rev. Lett. 63 (1989) 1849.
[2] H. Ohno, A. Shen, F. Matsukura, A. Oiwa, A. Endo, Y. lye, Appl. Phys. Lett. 69 (1996) 363.
[3] H. Ohno, Science 281 (1998) 951.
[4] S. Nakamura, M. Senoh, S. Nagahama, N. Iwasa, T. Yamada, T. Matsushita, H. Kiyoku, Y. Sugimoto, Jpn. J. Appl. Phys. Part 2 35 (1996) 217.
[5] I. Akasaki, S. Sota, H. Sakai, T. Tanaka, M. Koike, H. Amano, Electron. Lett. 32 (1996) 1105.
[6] R.P. Vaudo, I.K. Goepfert, T.D. Moustakas, D.M. Geyea, T.J. Frey, K. Meehan, J. Appl. Phys. 79 (1996) 2779.
[7] T. Dietl, H. Ohno, F. Matsukura, J. Cibert, D. Ferrand, Science 287 (2000) 1019.
[8] M.E. Overberg, C.R. Abernathy, S.J. Pearton, N.A. Theodoropoulou, K.T. McCarthy, A.F. Hebard, Appl. Phys. Lett. 79 (2001) 1312.
[9] M. Zajac, R. Doradzinski, J. Gosk, J. Szczytko, M. Lefeld-Sosnowaka, M. Kaminska, A. Twardowski, M. Placzewska, E. Grzanka, W. Gebicki, Appl. Phys. Lett. 78 (2001) 1276.
[10] M.L. Reed, N.A. El-Masry, H.H. Stadelmaier, M.K. Ritums, M.J. Reed, C.A. Parker, J.C. Roberts, S.M. Bedair, Appl. Phys. Lett. 79 (2001) 3473.
[11] Y.L. Soo, G. Kioseoglou, S. Kim, S. Huang, Y.H. Kao, S. Kuwabara, S. Owa, T. Kondo, H. Munekata, Appl. Phys. Lett. 79 (2001) 3926.
[12] S. Kuwabara, T. Kondo, T. Chikyow, P. Ahmet, H. Munekata, Jpn. J. Appl. Phys. 40 (2001) L724.
[13] W. Gebicki, J. Strzeszewski, G. Kamler, T. Szyszko, S. Podsiadlo, Appl. Phys. Lett 76 (2000) 3870.
[14] W. Limmer, W. Ritter, R. Sauer, B. Mensching, C. Liu, B. Rauschenbach, Appl. Phys. Lett. 72 (1998) 2589.
[15] L.S. Wang, S. Tripathy, W.H. Sun, S.J. Chua, J. Raman Spectrosc. 35 (2004) 73.
[16] V.Y. Davydov, Y.E. Kitaev, I.N. Goncharuk, A.N. Smimov, J. Graul, O. Semchinova, D. Uffman, M.B. Smirnov, A.P. Mirgorodsky, R.A. Evarestov, Phys. Rev. B 58 (1998) 12899.
[17] W. Gebicki, L. Adamowicz, J. Strzeszewski, S. Podsiado, T. Szyszko, G. Kamler, Mater. Sci. Eng. B 82 (2001) 182.
[18] A. Kaschner, H. Siegle, G. Kaczmarczyk, M. Straßburg, A. Hoffmann, C. Thomsen, U. Birkle, S. Einfeldt, D. Hommel, Appl. Phys. Lett. 74 (1999) 3281.
[19] G. Thaler, R. Frazier, B. Gilla, J. Stapleton, M. Davidson, C.R. Abernathey, S.J. Pearton, C. Segre, Appl. Phys. Lett. 84 (2004) 1314.
[20] S. Dhar, O. Brandt, A. Trampert, L. Daweriz, K.J. Friendland, K.H. Ploog, J. Keller, B. Beschoten, G. Guntherodt, Appl. Phys. Lett. 82 (2003) 2077.
[21] J.Y. Chang, G.H. Kim, J.M. Lee, S.H. Han, W.Y. Lee, M.H. Ham, K.S. Huh, J.M. Myoung, J. Appl. Phys. 93 (2003) 4512.
[22] J. Wang, Z. Li, W. Cai, Z. Miao, P. Chen, W. Lu, Appl. Phys. A 76 (2003) 975.